TABLE II
TEST REPORT OF MSOC-2 (TEST INPUT PINS = 4)

Test Session	Number of Clock cycles required in division-0	Number of Clock cycles required in division-1	Core (Cores) Tested during this test Session	Total clock cycles required to test this Mixed-Signal SoC-1
Session-0	50	95	Core1 and Core5	
Session-1	128	114	Core 0 and Core4	3335
Session-2	0	3048	Core3	
Session-3	0	78	Core2	

VIII. CONCLUSION

In this paper, an efficient implementation of a TAM is proposed for the MSOC testing. The technique introduces I/O access of the analog cores through the MTAM switch, which is introduced in the design. An integrated scheduling algorithm for MSOCs is proposed. The method is fully digitally compliant and, therefore, analog and digital cores can be tested in parallel. To test the algorithm, a CAT tool has been developed. A number of MSOCs have been designed using ISCAS'89 circuits for digital cores and ITC'97 circuits for analog cores. Results on these MSOCs show that the proposed method provides 100% fault coverage and offers a hardware-efficient integrated DFT solution.

REFERENCES

[1] S. Dey, E. J. Marinissen, and Y. Zorian, "Test access methodology for system-on-chip testing," *Testing System Chips: Methodologies and Experiences*, pp. 36–48, Sep. 1999.
[2] T. J. Chakraborty, S. Bhawmic, and C. H. Chiang, "Test access methodology for system-on-chip testing," in *Proc. IEEE Int. Workshop TECS*, Montreal, QC, Canada, May 2000, pp. 1.1–1.7.
[3] T. Vana and D. Blair, "Convergent SOCs challenge mixed-signal test," *Eval. Eng.*, 2000. [Online]. Available: http://www.evaluationengineering.com/archive/articles/0103ate.htm
[4] F. M. Bufler, Y. Asahi, H. Yoshimura, C. Zechner, A. Schenk, and W. Fichtner, "Monte Carlo simulation and measurement of nanoscale n-MOSFETs," *IEEE Trans. Electron Devices*, vol. 50, no. 2, pp. 418–424, Feb. 2003.
[5] J. C. Hamann, J. W. Pierre, S. F. Legowski, and F. M. Long, "Using Monte Carlo simulation to introduce tolerance design to undergraduates," *IEEE Trans. Educ.*, vol. 42, no. 1, pp. 1–7, Feb. 1999.
[6] A. Osseiran, *Analog and Mixed-Signal Boundary-Scan*. Norwell, MA: Kluwer, 1999.
[7] S. Basu, I. Sengupta, D. R. Chowdhury, and S. Bhowmik, "An integrated approach to testing embedded core and interconnects using test access mechanism (TAM) switch," *J. Electron. Test.: Theory Appl. (JETTA), Special Issue on Plug-and-Play Test Automation for System-on-a-Chip*, vol. 18, no. 4/5, pp. 475–485, Aug. 2002.
[8] A. Sehgal, S. Ozev, and K. Chakrabarty, "TAM optimization for mixed-signal SOCs using analog test wrappers," in *Proc. ICCAD*, San Jose, CA, Nov. 2003, pp. 95–99.

Orthonormal Bandlimited Kautz Sequences for Global System Modeling From Piecewise Rational Models

Luc Knockaert and Tom Dhaene

***Abstract*—Frequency-domain rational macromodeling techniques have to be limited to relatively small frequency ranges or to a limited number of poles, mostly due to numerical issues. A pertinent problem in system modeling is therefore to come up with a global broad-band macromodel, given a number of piecewise rational, possibly disjoint, small-band models. We describe an effective implementation procedure, based on orthonormal bandlimited Kautz sequences. As a first step, we show how a truncated Kautz basis can be obtained directly from a judiciously chosen state–space description. Next, having incorporated the bandlimitedness requirement, we obtain imbeddable orthonormal bandlimited Kautz sequences. A numerical procedure for calculating the underlying bandlimited scalar products and Grammians, as applied to piecewise bandlimited state–space data, is implemented and tested.**

***Index Terms*—Bandlimited functions, orthonormal bases, piecewise rational functions, state–space description, system modeling.**

I. INTRODUCTION

As the size of microwave and radio-frequency (RF) components decreases and the operation frequencies increase, efficient global broad-band macromodeling techniques become paramount for accurate frequency- and time-domain characterization and simulation of high-speed systems. Frequency-domain rational macromodeling techniques can be limited to relatively small frequency ranges or to a limited number of poles, often due to numerical issues. For example, adaptive frequency sampling (AFS) techniques, such as those in [1] and [2], build multiple piecewise rational bandlimited macromodels, based on a sparse set of computationally expensive simulation-based data samples. However, for circuit simulation purposes, global broad-band rational macromodels are required with validity in the overall frequency range.

A common approach to tackle the globality issue is to evaluate all small-band rational models at a large set of frequencies, and to use a stable rational approximation technique for frequency-domain identification of the overall system [3]. Unfortunately, a lot of up-front knowledge about the pole-zero behavior of the multiple rational models is usually lost while solving the system-identification problem. Other broad-band modeling techniques, such as complex frequency hopping (CFH) [4] and related methods [5], [6], do use information about the dominant stable poles, and allow pole clustering and pole relocation. Usually, these techniques use a lot of heuristic rules to build the broad-band models.

Here, we will pursue another avenue, based on complete orthonormal Kautz bases (COKBs). In recent years, pertinent research relating to COKB for use in continuous-time system modeling [7] and system identification [8] has appeared in the literature. The fundamental link of the COKB with the well-known Müntz–Szász completeness condition [9] generally allows for a better understanding of these uniformly bounded complete rational bases in Hardy space. However,

Manuscript received July 1, 2004; revised December 15, 2004 and May 4, 2005. This paper was recommended by Associate Editor L. M. Silveira.

L. Knockaert is with the Department Information Technology-Interuniversity Microelectronic Center (INTEC-IMEC), Ghent University, B-9000 Gent, Belgium (e-mail: knokaert@intec.ugent.be).

T. Dhaene is with the Electronic Design Automation Software (EEsof EDA) Division, Agilent Technologies, B-9000 Gent, Belgium, and also with the University of Antwerp, B-2020 Antwerp, Belgium.

Digital Object Identifier 10.1109/TCAD.2005.855888

a major drawback of the COKB, which will be remedied here, is that infinite frequency-domain knowledge is needed in order to calculate the pertinent scalar products, although of course, most often, in practice, one deals with essentially bandlimited functions and systems.

In this paper, a global wide-band rational macromodel is built, based on multiple piecewise, possibly disjoint, rational approximations. We follow a bandlimited least squares state–space COKB approach. As a first step, we show how truncated COKB can be obtained directly from a judiciously chosen state–space description. Next, having incorporated the bandlimitedness requirement in a more appropriate scalar product, we obtain orthonormal bandlimited Kautz sequences that are imbeddable in a more general Kautz description. Finally, a numerical procedure for calculating the underlying scalar products and bandlimited controllability Grammians, as applied to piecewise bandlimited state–space data, is implemented, and pertinent examples are presented.

The main strength and novelty of our approach resides in the fact that all poles of the underlying small-band models are efficiently reused, and that the resulting global state–space model presents smooth modeling in the transition regions between the different disjoint frequency bands. This makes the present method unique as compared with obvious resampling techniques, since one cannot resample in the transition regions for the simple reason that all sampling data there are actually missing. In other words, we perform extrapolation in the transition regions without resampling. Note that all broad-band macromodels should be passive and sufficiently compact, both for physical and efficiency reasons. Once the broad-band macromodels have been established, a passivity-enforcement postprocessing step, such as the ones presented in [10]–[13], and a passivity-preserving reduced-order modeling (ROM) step, such as the ones documented in [14]–[18], can be performed.

II. Truncated Kautz Basis

We work in the Hilbert space $L_2(R_+)$ of square integrable functions over $[0,\infty)$ with scalar product

$$(f|g)=\int_0^\infty f(t)\overline{g(t)}dt. \tag{1}$$

A closely associated Hilbert space is the Hardy space $\mathcal{H}_2$ consisting of all functions analytic in the open right halfplane $\Re s>0$ and square integrable over the imaginary axis with scalar product

$$\langle F|G\rangle=\frac{1}{2\pi}\int_{-\infty}^{\infty}F(i\omega)\overline{G(i\omega)}d\omega. \tag{2}$$

It is known [9] that the completeness of a sequence of stable exponentials $\{\mathrm{e}^{p_n t}\}$, $\Re(p_n)<0$ in $L_2(R_+)$ is equivalent with the Müntz–Szász condition

$$\sum_{n=0}^{\infty}\frac{-\Re(p_n)}{1+|p_n|^2}=\infty \tag{3}$$

where $\Re(p)$ stands for the real part of p. In $\mathcal{H}_2$, the Müntz–Szász condition (3) naturally governs the completeness of the pole system $\{1/(s-p_n)\}$. Note that the condition (3) remains valid for higher order poles $\{1/(s-p_n)^k\}$, corresponding with the modulated exponential $\{\mathrm{e}^{p_n t}t^{k-1}/(k-1)!\}$, if the sum in (3) is counted according to the multiplicity of the poles, which can even be infinite: For example, in the Laguerre COKB [9], there is only one pole of infinite multiplicity. In the sequel, for simplicity, we will assume only simple poles unless otherwise stated. The above pole system can be orthonormalized to yield the COKB

$$\Phi_n(s)=\frac{\sqrt{-2\Re(p_n)}}{s-p_n}\prod_{k=0}^{n-1}\left(\frac{s+\overline{p_k}}{s-p_k}\right),\qquad n=0,1,2,\ldots. \tag{4}$$

Given any function $F(s)$ in $\mathcal{H}_2$, we can therefore write down the expansion

$$F(s)=\sum_{n=0}^{\infty}f_n\Phi_n(s) \tag{5}$$

with $f_n=\langle F|\Phi_n\rangle$. If we truncate the sum to N terms, we obtain the real-rational[1] approximation

$$F_N(s)=\sum_{n=0}^{N-1}f_n\Phi_n(s). \tag{6}$$

However, a major drawback of the COKB is that it is not real rational in the presence of complex conjugate pole pairs. We therefore propose the following simple state–space method for obtaining a real-rational orthonormal Kautz segment. Let the $N\times N$ matrix A be the real canonical modal representation of the poles $\{p_0,p_1,\ldots,p_{N-1}\}$, that is, the real poles are diagonal elements of A, and the conjugate complex poles are 2×2 diagonal blocks of A of the form $[\Re p,\Im p;-\Im p,\Re p]$, resulting in an overall block-diagonal matrix A. Since any strictly proper rational function with these poles can be written in the state–space format $C^{\mathrm{T}}(sI-A)^{-1}B$, where C and B are column vectors and I is the identity matrix, we may express any sequence of would-be orthonormal rational functions $\phi_n(s)$ with these poles as

$$\phi_n(s)=C_n^{\mathrm{T}}(sI-A)^{-1}B. \tag{7}$$

For orthonormality, we require

$$\begin{aligned}&\frac{1}{2\pi}\int_{-\infty}^{\infty}C_n^{\mathrm{T}}(i\omega I-A)^{-1}B\left[C_m^{\mathrm{T}}(-i\omega I-A)^{-1}B\right]^{\mathrm{T}}d\omega\\&\quad=C_n^{\mathrm{T}}\left[\int_0^\infty \mathrm{e}^{At}BB^{\mathrm{T}}\mathrm{e}^{A^{\mathrm{T}}t}dt\right]C_m\\&\quad=C_n^{\mathrm{T}}W_\infty C_m=\delta_{n,m}\end{aligned} \tag{8}$$

where W_∞ is the controllability Grammian satisfying the Lyapunov equation

$$AW_\infty+W_\infty A^{\mathrm{T}}=-BB^{\mathrm{T}}. \tag{9}$$

It is well known that W_∞ is positive definite if and only if the pair (A,B) is controllable. In that case, from the Cholesky decomposition $W_\infty=D^TD$, we obtain that the sequence $\phi_n(s)$ is orthonormal, provided the vectors DC_n are orthonormal. The simplest way to do so is to take $DC_n=e_n$, where $e_n=(0\ldots1\ldots0)^{\mathrm{T}}$ is a unit column vector with 1 at position n. If we take A as the real canonical modal representation of the poles, considered all different, then in order to have a controllable (A,B) pair, it is sufficient to have a B vector with all its entries nonvanishing, say $B=\sum e_n$. With all this in mind,

[1]Real-rationality means that $F(s)$ is rational with $F(-i\omega)=\overline{F(i\omega)}$.

and given any function $F(s)$ in $\mathcal{H}_2$, it is an easy matter to obtain the rational approximation, with respect to the chosen poles:

$$F_N(s) = \sum_{n=0}^{N-1} \langle F|\phi_n\rangle \phi_n(s) = C_{F,N}^{\mathrm{T}}(sI - A)^{-1}B \tag{10}$$

where

$$C_{F,N} = \sum_{n=0}^{N-1} \langle F|\phi_n\rangle C_n. \tag{11}$$

III. Bandlimited Truncated Kautz Sequence

The main problem with the approach of the previous section is that the computations of the scalar products $\langle F|\phi_n\rangle$ require infinite band knowledge of $F(i\omega)$, which of course is not the case in practice. If we suppose that we dispose off data in a bandlimited window $-\alpha \le \omega \le \alpha$, we can tentatively try to replace $\langle F|G\rangle$ with

$$\langle F|G\rangle_\alpha = \frac{1}{2\pi}\int_{-\alpha}^{\alpha} F(i\omega)\overline{G(i\omega)}d\omega \tag{12}$$

but then of course the $\{\Phi_n(s)\}$ or $\{\phi_n(s)\}$ are no longer orthonormal with respect to this bandlimited scalar product. Fortunately, we have the following.

Theorem: Let the rational functions $\{\phi_n(s)\}$ be orthonormal with respect to $\langle F|G\rangle$. Then, the rational functions

$$\xi_n(s) = \phi_n\left(\frac{\alpha^2 s}{s^2+\alpha^2}\right)\frac{\alpha(s+\alpha)}{s^2+\alpha^2} \tag{13}$$

are orthonormal with respect to the bandlimited scalar product $\langle F|G\rangle_\alpha$.

Proof: We have

$$\frac{1}{2\pi}\int_{-\infty}^{\infty} \phi_n(i\omega)\overline{\phi_m(i\omega)}d\omega = \delta_{n,m}. \tag{14}$$

With the real change of variables $\omega = \alpha^2 u/(\alpha^2 - u^2)$, we obtain

$$\frac{1}{2\pi}\int_{-\alpha}^{\alpha} \phi_n\left(\frac{i\alpha^2 u}{\alpha^2-u^2}\right)\frac{\alpha(\alpha+iu)}{\alpha^2-u^2} \times \overline{\phi_m\left(\frac{i\alpha^2 u}{\alpha^2-u^2}\right)\frac{\alpha(\alpha+iu)}{\alpha^2-u^2}}du = \delta_{n,m} \tag{15}$$

and the proof is complete by putting $s = iu$. ∎

Note that, by means of the mapping (13), the COKB $\{\Phi_n(s)\}$ transforms into the α-bandlimited orthonormal sequence

$$\Xi_n(s) = \sqrt{-2\Re(p_n)}\frac{\alpha(s+\alpha)}{\alpha^2 s - p_n(s^2+\alpha^2)} \times \prod_{k=0}^{n-1}\left(\frac{\alpha^2 s + \overline{p_k}(s^2+\alpha^2)}{\alpha^2 s - p_k(s^2+\alpha^2)}\right). \tag{16}$$

It is seen that the poles $\{q_k\}$ of $\{\Xi_n(s)\}$ are found by solving $\alpha^2 s - (\alpha^2+s^2)p_k = 0$, and it is easy to show that the poles q_k obtained in this way are stable. As in the previous section, from $\phi_n(s) = C_n^{\mathrm{T}}(sI-A)^{-1}B$, we obtain the bandlimited counterparts

$$\xi_n(s) = \alpha(s+\alpha)C_n^{\mathrm{T}}\left(\alpha^2 sI - (\alpha^2+s^2)A\right)^{-1}B \tag{17}$$

which can be written in a state–space format of doubled dimension as

$$\xi_n(s) = \tilde{C}_n^{\mathrm{T}}(sI-\tilde{A})^{-1}\tilde{B} \tag{18}$$

with

$$\tilde{C}_n = \begin{pmatrix} C_n \\ C_n \end{pmatrix} \quad \tilde{B} = \begin{pmatrix} 0 \\ -\alpha A^{-1}B \end{pmatrix} \quad \tilde{A} = \begin{pmatrix} 0 & \alpha I \\ -\alpha I & \alpha^2 A^{-1} \end{pmatrix}. \tag{19}$$

It is seen that the formulation (17)–(19) is not easy to deal with. However, since the equation

$$\frac{\alpha^2 s}{s^2+\alpha^2} = \frac{\alpha^2 q}{q^2+\alpha^2} \tag{20}$$

admits both the pole $s = q$ and the reflected pole $s = \alpha^2/q$ as solutions, it is clear that the α-bandlimited orthonormal sequence $\{\Xi_n(s)\}$ can be imbedded in a COKB with poles $\{q_k\}$ and $\{\tilde{q}_k\} = \{\alpha^2/q_k\}$. Note also that when the set $\{q_k\}$ satisfies the Müntz–Szász condition, the set $\{\tilde{q}_k\}$ also does, and vice versa.

Hence, instead of taking $\tilde{A}$ as defined in (19), we take the $2N \times 2N$ matrix $\tilde{A}$ as the real canonical modal representation of the poles $\{q_0, \tilde{q}_0, q_1, \tilde{q}_1, \ldots, q_{N-1}, \tilde{q}_{N-1}\}$. The column vector $\tilde{B}$ of length $2N$ consists of only 1's, and the $2N$ column vectors $\tilde{C}_n$ are obtained by the orthonormalization procedure

$$\frac{1}{2\pi}\int_{-\alpha}^{\alpha} \tilde{C}_n^{\mathrm{T}}(i\omega I - \tilde{A})^{-1} \times \tilde{B}\tilde{C}_m^{\mathrm{T}}(-i\omega I - \tilde{A})^{-1}\tilde{B}d\omega = \tilde{C}_n^{\mathrm{T}} W_\alpha \tilde{C}_m = \delta_{n,m} \tag{21}$$

where W_α is the bandlimited controllability Grammian

$$W_\alpha = \frac{1}{2\pi}\int_{-\alpha}^{\alpha}(i\omega I - \tilde{A})^{-1}\tilde{B}\tilde{B}^{\mathrm{T}}(-i\omega I - \tilde{A}^{\mathrm{T}})^{-1}d\omega = \int_0^\infty\int_0^\infty \frac{\sin\alpha(t-\tau)}{\pi(t-\tau)} e^{\tilde{A}t}\tilde{B}\tilde{B}^{\mathrm{T}}e^{\tilde{A}^{\mathrm{T}}\tau}dt\,d\tau. \tag{22}$$

Calculation of the bandlimited controllability Grammian W_α can be effectively performed by the arccot recipe of the next section for calculating bandlimited scalar products, since we can write

$$W_\alpha = \left\langle (i\omega I - \tilde{A})^{-1}\tilde{B} \middle| \left[(i\omega I - \tilde{A})^{-1}\tilde{B}\right]^{\mathrm{T}} \right\rangle_\alpha. \tag{23}$$

In the same vein as the previous section, using only bandlimited data, and with $\tilde{\xi}_n(s) = \tilde{C}_n^{\mathrm{T}}(sI-\tilde{A})^{-1}\tilde{B}$, we obtain the rational approximation

$$F_{2N,\alpha}(s) = \sum_{n=0}^{2N-1} \langle F|\tilde{\xi}_n\rangle_\alpha \tilde{\xi}_n(s) = \tilde{C}_{F,2N}^{\mathrm{T}}(sI-\tilde{A})^{-1}\tilde{B} \tag{24}$$

where

$$\tilde{C}_{F,2N} = \sum_{n=0}^{2N-1} \langle F|\tilde{\xi}_n\rangle_\alpha \tilde{C}_n. \tag{25}$$

Actually, we do not need to calculate the orthonormal functions $\tilde{\xi}_n(s)$ beforehand, since $\tilde{C}_{F,2N}$ can alternatively be found by means of the minimization procedure

$$\tilde{C}_{F,2N} = \arg\min_{\tilde{C}} \left\langle F(i\omega) - \tilde{C}^{\mathrm{T}}(i\omega I - \tilde{A})^{-1}\tilde{B}|F(i\omega) - \tilde{C}^{\mathrm{T}}(i\omega I - \tilde{A})^{-1}\tilde{B}\right\rangle_\alpha. \tag{26}$$

From the standard quadratic minimization theory, we easily obtain

$$\tilde{C}_{F,2N} = W_\alpha^{-1}\Re\left\{\left\langle (i\omega - \tilde{A})^{-1}\tilde{B}|F(i\omega)\right\rangle_\alpha\right\}. \tag{27}$$

IV. Piecewise Bandlimited State–Space Data

Suppose we have piecewise bandlimited state–space data at our disposal, i.e.,

$$\begin{aligned} F(i\omega) &= \mathcal{F}_k(i\omega) \\ &= \mathcal{C}_k^{\mathrm{T}}(i\omega I - \mathcal{A}_k)^{-1}\mathcal{B}_k, \\ &\qquad 0 \le \gamma_k \le |\omega| \le \beta_k \quad k = 1, \ldots, M \end{aligned} \tag{28}$$

with $0 < \beta_k \le \gamma_{k+1}$ and $\beta_M = \alpha$. The objective is to obtain a unique rational approximation that well matches all the piecewise bandlimited functions $\mathcal{F}_k(i\omega)$ over the frequency range $[-\alpha, \alpha]$. By the theory of the previous section, in order to obtain the overall rational approximation $F_{2N,\alpha}(s)$, we first need to select an appropriate stable pole segment. A straightforward requirement is that one includes the set of all the stable poles of the matrices $\mathcal{A}_k$ in the $\{q_k\}$ pole sequence. To further enhance the dynamical range, this pole segment can be completed by a truncated sequence of other stable poles satisfying the Müntz–Szász condition, say, e.g., a sequence of equal Laguerre poles $\{-\alpha; k = 1, \ldots, L\}$, or even better, to avoid degeneracy problems, a sequence of the form $\{-k\alpha/(k+1); k = 1, \ldots, L\}$. Finally, the reflected poles α^2/q_k are appended to yield the full pole segment, which enables the construction of the canonical modal system matrix.

Next, we need to calculate the scalar products $\langle F|\tilde{\xi}_n\rangle_\alpha$. After splitting the integrals, we obtain

$$\langle F|\tilde{\xi}_n\rangle_\alpha = \sum_{k=1}^{M}\left\{\langle \mathcal{F}_k|\tilde{\xi}_n\rangle_{\beta_k} - \langle \mathcal{F}_k|\tilde{\xi}_n\rangle_{\gamma_k}\right\}. \tag{29}$$

Since $\mathcal{F}_k$ and $\tilde{\xi}_n$ both admit standard state–space representations, it is seen that the obtention of $\langle F|\tilde{\xi}_n\rangle_\alpha$ boils down to the calculation of

$$\begin{aligned} \langle F_1|F_2\rangle_\alpha &= \frac{1}{2\pi}\int_{-\alpha}^{\alpha} C_1^{\mathrm{T}}(i\omega I - A_1)^{-1}B_1\overline{C_2^{\mathrm{T}}(i\omega I - A_2)^{-1}B_2}d\omega \\ &= \frac{1}{2\pi}\int_{-\alpha}^{\alpha} C_{12}^{\mathrm{T}}(i\omega I - A_{12})^{-1}B_{12}d\omega \end{aligned} \tag{30}$$

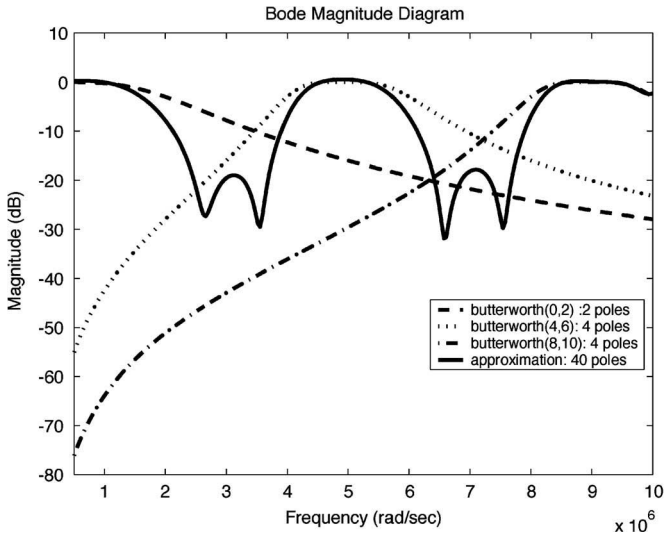

Fig. 1. Bode magnitude plot for the Butterworth cascade example.

where

$$C_{12} = \begin{pmatrix} 0 \\ C_2 \end{pmatrix} \quad B_{12} = \begin{pmatrix} B_1 \\ 0 \end{pmatrix} \quad A_{12} = \begin{pmatrix} A_1 & 0 \\ -B_2C_1^{\mathrm{T}} & -A_2 \end{pmatrix}. \tag{31}$$

Since

$$\frac{1}{2\pi}\int_{-\alpha}^{\alpha}\frac{d\omega}{i\omega - z} = -\frac{1}{\pi}\mathrm{arccot}\left(\frac{z}{\alpha}\right), \qquad \Re z \neq 0 \tag{32}$$

we finally obtain

$$\langle F_1|F_2\rangle_\alpha = -\frac{1}{\pi}C_{12}^{\mathrm{T}}\mathrm{arccot}\left(\frac{A_{12}}{\alpha}\right)B_{12}. \tag{33}$$

The calculation of $\mathrm{arccot}(A)$, where A is any real matrix, is based on a method of Parlett for the calculation of functions of matrices [19].

Last but not least, as a consequence of the typical construction of the $\tilde{A}$ matrix, the resulting rational function $F_{2N,\alpha}(s) = \tilde{C}_{F,2N}^{\mathrm{T}}(sI - \tilde{A})^{-1}\tilde{B}$ may present a too-large model order (number of poles). Therefore, the state–space representation of $F_{2N,\alpha}(s)$ may be inputted to a typical ROM algorithm to obtain a model of sufficiently low order. Finally, for physical consistency, a passivity-enforcement step may be considered.

V. Numerical Simulations

A. Butterworth Filters

We consider a parallel cascade (union of passbands) of three disjoint Butterworth filters: The first is two-pole low pass with cutoff $\omega_c = 2.0\text{e}6$ rad/s, the second is four-pole bandpass in $4.0\text{e}6$ rad/s $\le \omega \le 6.0\text{e}6$ rad/s, and the third is four-pole bandpass in $8.0\text{e}6$ rad/s $\le \omega \le 1.0\text{e}7$ rad/s. The purpose is of course to find a global state–space model that is sufficiently close to each of the three filters in their respective frequency bands. The global bandwidth is $\alpha = 1.0\text{e}7$ rad/s and the number of stable poles is 10. Adding ten approximate Laguerre poles $\{-\alpha/2, -2\alpha/3, \ldots, -10\alpha/11\}$ and reflecting the poles by means of the transformation α^2/p results in a total of 40 system poles to work with. Applying the theory of the previous sections results in the obtention of $\tilde{C}_{F,2N}$ and the global state–space description. A Bode magnitude diagram is shown in Fig. 1. Finally, as shown in Fig. 2, after

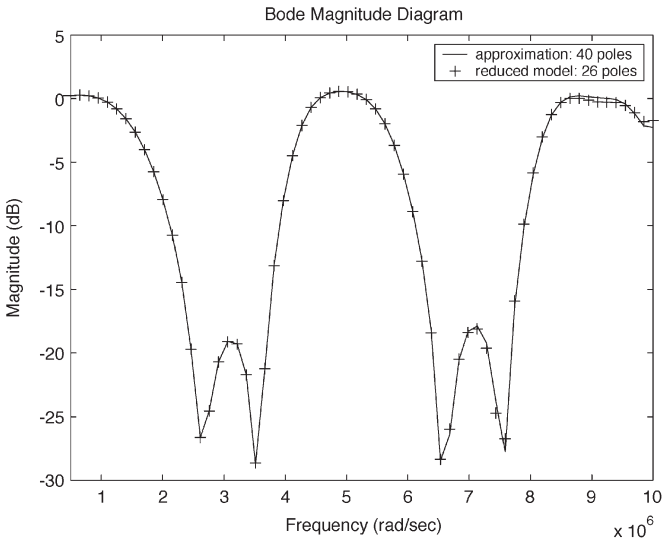

Fig. 2. Reduced-order model Bode magnitude plot for the Butterworth cascade example.

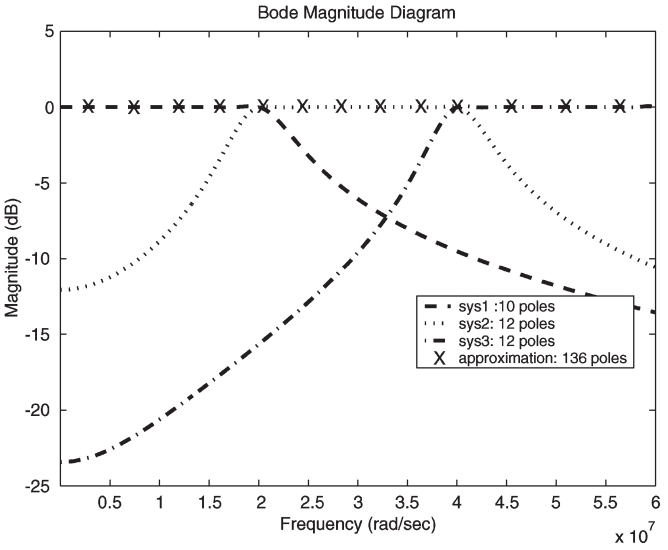

Fig. 3. Bode magnitude plot for the Neville-type pure-delay example.

a last Laguerre-Singular Value Decomposition (SVD) ROM step [16], we obtain an accurate reduced-order model with 26 system poles.

B. Bandlimited Interpolation

Sometimes a Neville-type rational interpolation procedure such as the Bulirsch–Stoer algorithm [20] can be used to find a rational function that is close to a tabulated function over a certain frequency range. A convenient version of this algorithm, different although similar to the one presented in [2], is as follows.

Consider a frequency response table $h = \{H_1, \overline{H_1}, \ldots, H_N, \overline{H_N}\}$ at the complex frequencies $\{s_1 = i\omega_1, s_2 = -i\omega_1, \ldots, s_{2N-1} = i\omega_N, s_{2N} = -i\omega_N\}$, with $0 < \omega_1 < \cdots < \omega_N < \infty$. Then, a real-rational function $R_{2N}(s) = a_{2N}(s)/b_{2N}(s)$ with N poles and $N-1$ zeros, such that $R_{2N}(s_k) = h_k$, can be constructed by the Neville-type algorithm

$$a_k(s) = \sigma_k a_{k-1}(s) + (s - s_{k-1})a_{k-2}(s) \tag{34}$$

$$b_k(s) = \sigma_k b_{k-1}(s) + (s - s_{k-1})b_{k-2}(s) \tag{35}$$

with initial values $a_0 = 0$, $a_1 = h_1$, $b_1 = b_0 = 1$. The value for σ_k is found by requiring that $h_k = a_k(s_k)/b_k(s_k)$, i.e.,

$$\sigma_k = (s_{k-1} - s_k)\frac{h_k b_{k-2}(s_k) - a_{k-2}(s_k)}{h_k b_{k-1}(s_k) - a_{k-1}(s_k)}. \tag{36}$$

It would be nice if the above interpolation algorithm also exhibited some extrapolation power, but unfortunately, in practice, this is rarely the case. For the obtention of a rational approximant of a given analytic function over a large bandwidth, we therefore need to interpolate over different relatively narrowbands, and afterwards combine the approaches in an overall rational model.

As an example, consider the pure-delay transfer function $\mathrm{e}^{-s\tau}$ with $\tau = 1\ \mu$s. Applying the Neville-type algorithm on equispaced samples in the bands $0 < \omega \leq 2.0\mathrm{e}7$ rad/s, $2.0\mathrm{e}7$ rad/s $\leq \omega \leq 4.0\mathrm{e}7$ rad/s, and $4.0\mathrm{e}7$ rad/s $\leq \omega \leq 6.0\mathrm{e}7$ rad/s, we obtain rational interpolants with, respectively, 10, 12, and 12 poles. The global bandwidth is $\alpha = 6.0\mathrm{e}7$ rad/s and the number of stable poles is 34. Adding 34 approximate Laguerre poles $\{-\alpha/2, -2\alpha/3, \ldots, -34\alpha/35\}$ and reflecting the poles results in a total of 136 system poles to process. Applying the theory of the previous sections results in the obtention of $\tilde{C}_{F,2N}$ and the global state–space description. A Bode magnitude diagram is shown in Fig. 3. We obtain an accurate reduced-order model with 72 system poles after performing an additional Laguerre-SVD ROM step, as seen in Fig. 4. As a last postprocessing step, a passivity-enforcement technique, such as the ones documented in [10]–[13], may be performed to obtain a physically correct model.

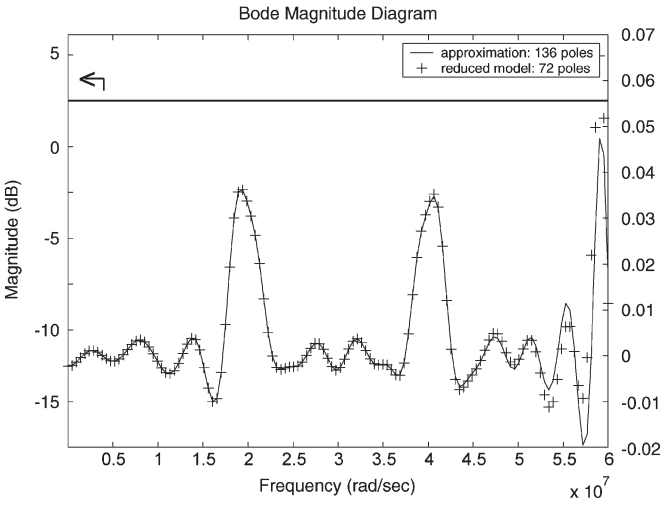

Fig. 4. Reduced-order model Bode magnitude plot for the Neville-type pure-delay example: The horizontal line at 0 dB with respect to the left decibel scale has been magnified to yield the nontrivial plot with respect to the right decibel scale.

VI. Conclusion

We have proposed a bandlimited least squares state–space-based approach in order to come up with a global system model, given different rational models in selected frequency subranges. We have shown how truncated Kautz bases can be obtained directly from a judiciously chosen local state–space description. Next, having incorporated the local bandlimitedness requirement, we have obtained orthonormal bandlimited Kautz sequences imbeddable in a more general Kautz description. Numerical procedures for the calculation of the underlying bandlimited controllability Grammians, as applied to piecewise bandlimited state–space data, have been implemented, and the Laguerre-SVD ROM algorithm has been utilized to further compress

the resulting global state–space model. Pertinent examples include the construction of a three-band parallel cascade of Butterworth filters, and the realization of a global system model for a pure-delay transfer function given bandlimited interpolation data in three different frequency bands. Passivity-enforcement techniques can be performed in a postprocessing step.

REFERENCES

[1] T. Dhaene, J. Ureel, N. Fache, and D. De Zutter, "Adaptive frequency sampling algorithm for fast and accurate S-parameter modeling of general planar structures," in *IEEE MTT-S Int. Microwave Symp. Dig.*, Orlando, FL, May 1995, vol. 3, pp. 1427–1430.

[2] R. Lehmensiek and P. Meyer, "An efficient adaptive frequency sampling algorithm for model-based parameter estimation as applied to aggressive space mapping," *Microw. Opt. Technol. Lett.*, vol. 24, no. 1, pp. 71–78, Jan. 2000.

[3] R. Pintelon and J. Schoukens, *System Identification, A Frequency Domain Approach*. New York: IEEE Press, 2001.

[4] E. Chiprout and M. S. Nakhla, "Analysis of interconnect networks using complex frequency hopping," *IEEE Trans. Comput.-Aided Des. Integr. Circuits Syst.*, vol. 14, no. 2, pp. 186–200, Feb. 1995.

[5] S.-H. Min and M. Swaminathan, "Construction of broadband passive macromodels from frequency data for simulation of distributed interconnect networks," *IEEE Trans. Electromagn. Compat.*, vol. 46, no. 4, pp. 544–558, Nov. 2004.

[6] J. Choi, S.-H. Min, J.-H. Kim, M. Swaminathan, W. Beyene, and X. Yuan, "Modeling and analysis of power distribution networks for Gigabit applications," *IEEE Trans. Mobile Comput.*, vol. 2, no. 4, pp. 299–313, Oct.–Dec. 2003.

[7] H. Akçay and B. Ninness, "Orthonormal basis functions for modelling continuous-time systems," *Signal Process.*, vol. 77, no. 3, pp. 261–274, Sep. 1999.

[8] B. Wahlberg, "System identification using Kautz models," *IEEE Trans. Autom. Control*, vol. 39, no. 6, pp. 1276–1281, Jun. 1994.

[9] L. Knockaert, "On orthonormal Müntz-Laguerre filters," *IEEE Trans. Signal Process.*, vol. 49, no. 4, pp. 790–793, Apr. 2001.

[10] B. Gustavsen and A. Semlyen, "Enforcing passivity for admittance matrices approximated by rational functions," *IEEE Trans. Power Syst.*, vol. 16, no. 1, pp. 97–104, Feb. 2001.

[11] D. Saraswat, R. Achar, and M. Nakhla, "A fast algorithm and paractical considerations for passive macromodeling of measured/simulated data," in *Proc. Topical Meeting Electrical Performance Electronic Packaging (EPEP)*, Monterey, CA, 2002, pp. 297–300.

[12] C. P. Coelho, J. R. Phillips, and L. M. Silveira, "A convex programming approach for generating guaranteed passive approximations to tabulated frequency data," *IEEE Trans. Comput.-Aided Des. Integr. Circuits Syst.*, vol. 23, no. 2, pp. 293–301, Feb. 2004.

[13] S. Grivet-Talocia, "Passivity enforcement via perturbation of Hamiltonian matrices," *IEEE Trans. Circuits Syst. I, Reg. Papers*, vol. 51, no. 9, pp. 1755–1769, Sep. 2004.

[14] P. Feldmann and R. W. Freund, "Efficient linear circuit analysis by Pade approximation via the Lanczos process," *IEEE Trans. Comput.-Aided Des. Integr. Circuits Syst.*, vol. 14, no. 5, pp. 639–649, May 1995.

[15] A. Odabasioglu, M. Celik, and L. T. Pileggi, "PRIMA: Passive reduced-order interconnect macromodeling algorithm," *IEEE Trans. Comput.-Aided Des. Integr. Circuits Syst.*, vol. 17, no. 8, pp. 645–654, Aug. 1998.

[16] L. Knockaert and D. De Zutter, "Laguerre-SVD reduced order modeling," *IEEE Trans. Microw. Theory Tech.*, vol. 48, no. 9, pp. 1469–1475, Sep. 2000.

[17] J. R. Phillips, L. Daniel, and L. M. Silveira, "Guaranteed passive balancing transformations for model order reduction," *IEEE Trans. Comput.-Aided Des. Integr. Circuits Syst.*, vol. 22, no. 8, pp. 1027–1041, Aug. 2003.

[18] L. Daniel, O. C. Siong, L. S. Chay, K. H. Lee, and J. White, "A multiparameter moment-matching model-reduction approach for generating geometrically parameterized interconnect performance models," *IEEE Trans. Comput.-Aided Des. Integr. Circuits Syst.*, vol. 23, no. 5, pp. 678–693, May 2004.

[19] G. H. Golub and C. F. Van Loan, *Matrix Computations*, 3rd ed. Baltimore, MD: The Johns Hopkins Univ. Press, 1996.

[20] W. H. Press, S. A. Teukolsky, W. T. Vetterling, and B. P. Flannery, *Numerical Recipes in Fortran, The Art of Scientific Computing*, 2nd ed. Cambridge, U.K.: Cambridge Univ. Press, 1992.

Arithmetic Transforms for Compositions of Sequential and Imprecise Datapaths

Katarzyna Radecka and Zeljko Zilic

***Abstract*—This paper addresses the issue of obtaining compact canonical representations of datapath circuits with sequential elements for the purpose of equivalence checking and component matching. First, the authors demonstrate the mechanisms for an efficient compositional construction of the arithmetic transform (AT), which is the underlying function representation used in modern word-level decision diagrams (WLDDs). Second, presented is a way of generating the canonical transforms of the sequential and imprecise datapath circuits.**

***Index Terms*—Arithmetic transform (AT), hardware verification, imprecise arithmetic, sequential circuits.**

I. INTRODUCTION

Arithmetic datapath circuits have always been important in the development of circuit representations suitable for formal verification. Early bit-level methods, including the binary decision diagram (BDD), proved to be insufficient in describing common arithmetic circuits like multipliers. The emergence of word-level decision diagrams (WLDDs) overcame this problem to some extent. Indeed, the interest in the verification of arithmetic circuits has been renewed [1]–[3]. Therefore, there is a shift in interest from bit-level to word-level forms. However, some caution is in place, as not all word-level representations are beneficial for arithmetic circuits. Good candidates are the descriptions based on the arithmetic transform (AT) [4], such as binary moment diagrams (BMDs) [5], [6] and their extensions [7] that are compact for common arithmetic circuits.

This paper aims at enhancing the capability of basic AT forms. To reduce the complexity and to capitalize on the block-level structure, we consider the means to compose AT descriptions from those of the smaller blocks. However, unlike bit-level representations, the existing AT-based word-level forms cannot be composed because of the data-type incompatibility—the inputs are binary, while the outputs are word-level quantities. To address this problem, we propose AT extensions that facilitate the combination of ATs describing the combinational, sequential, and imprecise arithmetic blocks. We notice that the recently introduced Taylor expansion diagrams (TEDs) [8] also have basic composition properties, making the addition and multiplication of two TEDs feasible although apparently not simple [9].

Sequential elements in datapaths present another difficulty for word-level forms, which are only suitable for combinational functions. In general, the notion of a sequential equivalence [10] becomes fairly complex when allowing for manipulations such as retiming, pipelining, and FSM optimization. In this paper, we provide an extension to the AT for sequential datapaths. Using these forms, we show, for instance, how to match a specification with the sequential implementation in circuits employing distributed arithmetic (DA).

The final issue explored in this paper is the representation of imprecise arithmetic circuits. The major challenge here lays in the assertion of circuit correctness under the presence of an error due to the arithmetic imprecision. Imprecision naturally comes from the

Manuscript received October 6, 2004; revised February 7, 2005 and May 9, 2005. This paper was recommended by Associate Editor R. F. Damiano.

K. Radecka is with Concordia University, Montreal, QC H3G 1M8, Canada.

Z. Zilic is with McGill University, Montreal, QC H3A 2A7, Canada (e-mail: zeljko@ece.mcgill.ca).

Digital Object Identifier 10.1109/TCAD.2005.855935